Proc. Natl. Acad. Sci. USA
Vol. 85, pp. 1189–1193, February 1988
Immunology

Doxorubicin conjugated with a monoclonal antibody directed to a human melanoma-associated proteoglycan suppresses the growth of established tumor xenografts in nude mice

(immunotherapy of human melanoma/immunoconjugates)

HSIN MING YANG* AND RALPH A. REISFELD

Department of Immunology, Scripps Clinic and Research Foundation, 10666 North Torrey Pines Road, La Jolla, CA 92037

Communicated by M. Frederick Hawthorne, October 14, 1987

ABSTRACT **Doxorubicin (DXR) was covalently conjugated to a monoclonal antibody (mAb), 9.2.27 (IgG2a), which recognizes a chondroitin sulfate proteoglycan expressed preferentially on the surface of human melanoma cells. Immunoconjugates with a molar ratio of DXR to mAb ranging from 2:1 to 10:1 were obtained by coupling the drug via an acid-sensitive linker, *cis*-aconitic anhydride. The immunoreactivity of mAb 9.2.27 was well retained after conjugation. DXR–mAb 9.2.27 conjugates were found to be 2 orders of magnitude more potent in killing tumor cells *in vitro* (IC_{50} = 0.1 μM) than free drug targeted to drug receptors(s). Most significantly, DXR–mAb 9.2.27 immunoconjugates specifically suppressed the growth of established tumors *in vivo* and prolonged the life-span of tumor-bearing nude mice. This suppression of melanoma growth achieved by the immunoconjugate was both tumor and antibody specific. A biodistribution study indicated that DXR–mAb 9.2.27 conjugates delivered at least 4 times more DXR (3.7% total injected dose per g of tumor) as compared to free DXR alone (0.8% total injected dose per g of tumor) in tumor-bearing nude mice 48 hr postinjection. The tumor-suppressive effects of DXR–mAb 9.2.27 conjugates are even more remarkable since free DXR did not suppress tumor growth *in vivo* and also because this drug *per se* is known to be quite ineffective for the treatment of human melanoma.**

The potential usefulness of monoclonal antibodies (mAbs) to deliver drugs, radionuclides, or toxins to tumor sites *in vivo* has been under active investigation (1–3). mAbs directed against well-characterized tumor-associated antigens have made it possible to critically evaluate their suitabilities as carriers for cytotoxic molecules or radionuclides. The use of such immunoconjugates for accurate delivery of lethal agents to human tumor targets promises to create a generation of treatment modalities that may reduce side effects, facilitate more selective tumor targeting, result in improved therapeutic indices and decreased lethal doses, and possibly even decrease the incidence of multiple drug resistance.

Specifically, mAb 9.2.27, recognizing a melanoma-associated chondroitin sulfate proteoglycan expressed preferentially on the cell surface of human melanoma cells (4), was previously shown to only partially suppress the human melanoma xenograft in nude mice when conjugated with a diphtheria toxin A chain (5). In this report, we conjugated a chemotherapeutic drug, doxorubicin (DXR), to mAb 9.2.27 via an acid-sensitive linker, *cis*-aconitic anhydride. This linker between the macromolecule and the drug was reported to preserve both antibody and DXR activities (6, 7). It is postulated that such conjugates remain stable at the intravascular pH of 7.4, but once endocytosed by the target cell, the drug is cleaved in the more acidic environment of endosomes and lysosomes and intercalated with nuclear DNA (8–10). The results of our study showed that such immunoconjugates not only retained good immunoreactivity and pharmacological activity *in vitro* but also effectively suppressed established human melanoma xenografts in an athymic (nu/nu) mouse model.

The publication costs of this article were defrayed in part by page charge payment. This article must therefore be hereby marked "*advertisement*" in accordance with 18 U.S.C. §1734 solely to indicate this fact.

MATERIALS AND METHODS

Cells. UCLA-SO-M21 melanoma cells (M21) were maintained *in vitro* as described (4, 5). Neuroepithelioma cells (NMB-7) kindly provided by S. K. Liao (McMaster University, Canada) and adenocarcinoma of the lung cells (UCLA-SO-P3; UCLA-P3) were maintained in culture.

Antibodies. mAb 9.2.27 (IgG2a) recognizes a proteoglycan preferentially expressed on human melanoma cells (4). mAb 11.4.1 (IgG2a), directed against a mouse H-$2K^k$ antigen, was obtained from American Type Culture Collection. mAbs were purified by protein A-Sepharose chromatography (11).

Conjugation of DXR to mAbs. Conjugation of DXR to mAbs was achieved by an acid-sensitive linker, *cis*-aconitic anhydride, with modifications (6, 7). Briefly, 12 mg of *cis*-aconitic anhydride (Sigma) was dissolved in 3 ml of a 50% aqueous solution of *p*-dioxane at 25°C and added dropwise to an ice-cold solution of DXR (12 mg in 6 ml of distilled water) and keeping the pH at 9.0 by the addition of 0.5 M NaOH. After 15 min, the pH was adjusted to 7.0 and continued for another 1 hr. Six milligrams of 1-ethyl-3-(3-dimethylaminopropyl)carbodiimide (Sigma) was then added to the solution for 30 min, followed by 6 mg of mAb (10 mg/ml in P_i/NaCl, pH 7.0). The reaction proceeded at pH 7.0 for 3 hr at 25°C. The immunoconjugates were purified with Sephadex G-25 Fine (Pharmacia) and dialyzed against P_i/NaCl at 4°C. The molar ratio of mAb to DXR was determined by assessing protein concentration with a protein dye-binding assay (Bio-Rad) (12) while DXR was quantitated by measuring its absorbance at 476 nm with an extinction coefficient $\varepsilon^{1\%}_{1\ cm}$ of 173. The immunoconjugates were lyophilized in the presence of 10% lactose and were stored at −20°C until use.

ELISA. The retention of mAb activity after conjugation was determined with an ELISA as described (13). Antibody concentration was varied from 10 μg/ml to 10 ng/ml. The absorbance at 490 nm was measured with a microtiter plate reader (Bio-tek Instruments, Burlington, VT).

Growth Inhibition Achieved by DXR–mAb Conjugates. The pharmacological activity of DXR–mAb conjugates was assessed by a [^{3}H]thymidine incorporation assay. Briefly, 3×10^4 cells were exposed to serially diluted DXR–mAb for 2 hr at 25°C. The cells were then washed twice, plated into

Abbreviations: DXR, doxorubicin; mAb, monoclonal antibody.
*To whom reprint requests should be addressed.

96-well tissue culture plates (10^4 cells per well), and incubated at 37°C overnight in RPMI 1640 medium supplemented with 10% fetal calf serum. Subsequently, 1 μCi of [^{3}H]thymidine (1 Ci = 37 GBq) (New England Nuclear) was added to each well followed by incubation for another 24 hr. Cells were harvested, and the incorporation of [^{3}H]thymidine was determined. In these experiments, equivalent amounts of either native antibody or free DXR was added for comparison. NMB-7 neuroepithelioma cells served as an antigen-negative control, since they do not express the melanoma-associated proteoglycan antigen recognized by mAb 9.2.27.

Localization of DXR in M21 Cells. M21 melanoma (10^4 cells) were plated in a culture dish (Falcon 3001) overnight at 37°C in complete RPMI 1640 medium supplemented with 10% fetal calf serum. One milliliter of DXR–mAb 9.2.27 conjugate (50 μg of protein per ml) was added and incubated at 37°C from 30 min up to 3 hr. Unbound DXR–mAb conjugate was removed by washing twice with cold P_i/NaCl. Two milliliters of cold P_i/NaCl was added to the dish and the cells were examined with an ACAS 470 workstation (Meridian Instruments, Okemos, MI) equipped with a 514-nm Ar laser to excite the DXR molecules and measure the emissions of red fluorescence above 544 nm. In these experiments, the laser power was set at 200 mW and the efficiency of the photomultiplier tube was held at 50% with the scan strength set at 10% of original laser power. A pseudocolor image of fluorescent intensity was then generated. The corresponding phase-contrast image of the cells was taken directly from an Olympus OM inverted microscope. In some experiments, 25 μM chloroquine was added to the culture dishes for 1 hr at 37°C before adding the DXR–mAb conjugates containing an equal concentration of chloroquine.

Evaluation of the Efficacy of DXR–mAb Conjugates *in Vivo*. The efficacy and specificity of DXR–mAb 9.2.27 conjugates were analyzed in a xenogenic athymic (nu/nu) mouse model. Briefly, 5×10^6 M21 (antigen-positive) or UCLA-P3 (antigen-negative) cells were injected s.c. into the right flank of 6- to 8-wk-old female BALB/c (nu/nu) mice and allowed to establish a tumor for 10 and 8 days, respectively. Nude mice that had developed palpable tumors with tumor volumes of ≈10 mm^3 were then selected for treatments. A DXR–mAb 9.2.27 conjugate with a molar ratio of 10:1 was used for injection. Various treatment modalities were used including the following: mAb 9.2.27 alone, DXR alone, DXR–mAb 9.2.27 conjugate, mAb 9.2.27 mixed with an equal amount of DXR used in the DXR–mAb 9.2.27 conjugate, and an irrelevant DXR–mAb 11.4.1 conjugate. All injections were made i.v. at day 10 and at 3-day intervals thereafter for 30 days (10 injections). Each group contained 6–12 mice. Each animal received a total equivalent dose of 75 μg of DXR and/or 2 mg of mAb. Tumor growth was determined every 3rd day by measuring 3 diameters of the subcutaneous tumors with calipers. The tumor volume was calculated by the formula $(d_1 \times d_2 \times d_3)/2$ (14), where d_1, d_2, and d_3 are the length, width, and height of the tumor, respectively. The differences in tumor volumes between experimental groups were analyzed by the Student's t test. The median survival time in days was determined, and from this the percentage of increase in life-span (ILS) was calculated (15):

$$\%\text{ILS} = (t/c - 1) \times 100,$$

where t is the median survival days of mice in the experimental group treated with mAb 9.2.27–DXR and c is the median survival days of mice in the control group treated with mAb 9.2.27 alone.

Biodistribution of DXR–mAb 9.2.27 Conjugates. The respective tissue distributions of DXR *per se* and DXR–mAb 9.2.27 conjugates after i.v. injection were compared in nude mice bearing M21 tumors. Briefly, 10 μCi of [14-^{14}C]DXR (56 mCi/mmol; Amersham) or 5 μCi of [14-^{14}C]DXR–mAb 9.2.27 (1 μCi per mmol of conjugates) was injected i.v. through the tail vein into 12 mice with an average tumor weight of 400 mg. At 1, 6, 24, and 48 hr postinjection, three mice were bled retroorbitally, and major tissues were dissected, weighed, and dissolved in 4 ml of TS-2 (RPI, Mount Prospect, IL). The dissolved tissue was acidified and counted in a β-counter. The results were expressed as the percentage of injected dose per g of tissue.

RESULTS

Immunoreactivity of DXR–mAb 9.2.27 Conjugates. mAb 9.2.27 conjugated with 10 molar substitutions of DXR retained at least 80% of immunoreactivity after conjugation when measured by direct binding of mAb 9.2.27 or DXR–mAb 9.2.27 to M21 target cells in an ELISA (data not shown).

Pharmacological Activity of DXR–mAb 9.2.27 Conjugates. The DXR activity of immunoconjugates was monitored by an assay measuring [^{3}H]thymidine incorporation since DXR is known to intercalate with DNA (16) and cause a cell-cycle arrest in the G_2 phase (17). DXR–mAb 9.2.27 conjugates with a molar ratio of 10:1 (drug/Ab) showed specific dose-dependent growth inhibition of M21 target cells (9.2.27-positive; Fig. 1*A*) but had no effect at all on NMB-7 neuroepithelioma cells (9.2.27-negative; Fig. 1*B*). A 2-hr exposure of M21 cells to 8 μM DXR–mAb 9.2.27 conjugate inhibited 66% of the [^{3}H]thymidine incorporation as compared to a medium control (IC_{50} = 0.1 μM). Free DXR ranging from 10 nM to 1 μM had a negligible effect on [^{3}H]thymidine incorporation (IC_{50} = 10 μM). At corresponding concentrations, mAb 9.2.27 alone failed to inhibit the [^{3}H]thymidine incorporation (data not shown).

Specific Inhibition of Tumor Cell Growth by DXR–mAb Conjugates. To determine whether the observed effect of

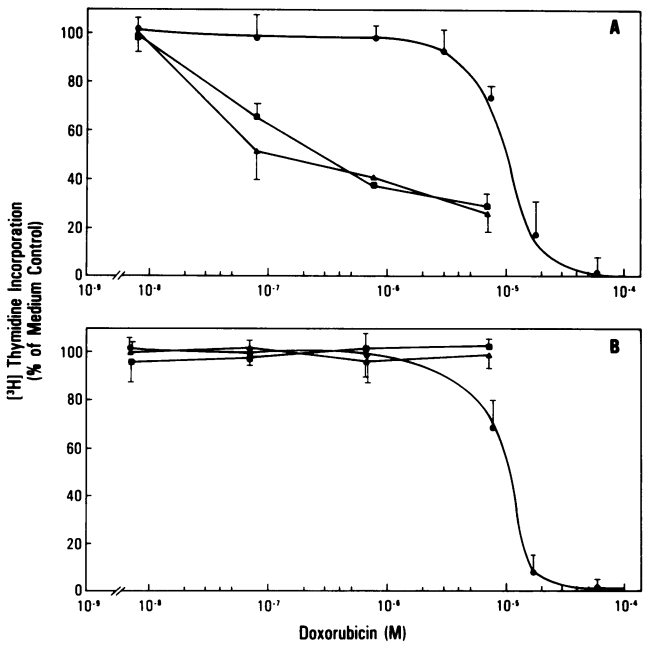

FIG. 1. Suppression of human tumor-cell growth *in vitro* by DXR–mAb 9.2.27 conjugates. The efficacy of two DXR–mAb 9.2.27 conjugates with molar DXR/mAb ratios of 10:1 (▲) and 5:1 (■) is shown in inhibiting [^{3}H]thymidine incorporation on 9.2.27 antigen-positive M21 cells (*A*) and 9.2.27 antigen-negative NMB-7 cells (*B*). Efficacy of DXR alone is also indicated (●). Each data point represents an average of triplicate determinations. At corresponding concentrations, mAb 9.2.27 alone fails to inhibit the incorporation of [^{3}H]thymidine (data not shown).

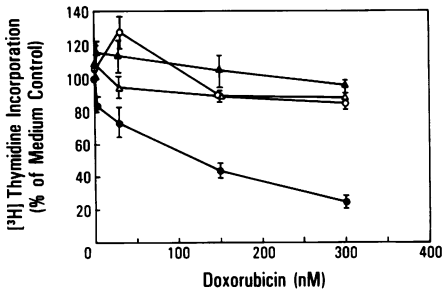

FIG. 2. Specificity of DXR–mAb conjugates in suppressing the growth of tumor cells *in vitro*. Equivalent doses of DXR in respective conjugates with mAb 9.2.27 (●), mAb 11.4.1 (▲), and normal mouse IgG (○) and of free DXR (△) were tested for their ability to inhibit the [³H]thymidine incorporation on M21 cells. Each data point represents an average of triplicate determinations.

DXR–mAb 9.2.27 conjugates (Fig. 1) is antigen specific, both an irrelevant mAb, 11.4.1 (IgG2a) directed against a mouse H-2K^k antigen, and a normal mouse IgG were conjugated to DXR using the same protocol as for mAb 9.2.27 (IgG2a). Results showed that at equivalent doses of DXR, only DXR–mAb 9.2.27 conjugates inhibited proliferation of M21 cells (Fig. 2). In contrast, DXR conjugated to either irrelevant mAb 11.4.1 or normal mouse IgG failed to achieve any significant inhibition of tumor cell growth.

Intracellular Localization of DXR–mAb Conjugates. To obtain some insight into possible mechanism(s) of growth inhibition achieved by DXR–mAb conjugates, the intracellular localization of DXR–mAb conjugates was monitored with an ACAS workstation. In an initial study, free DXR

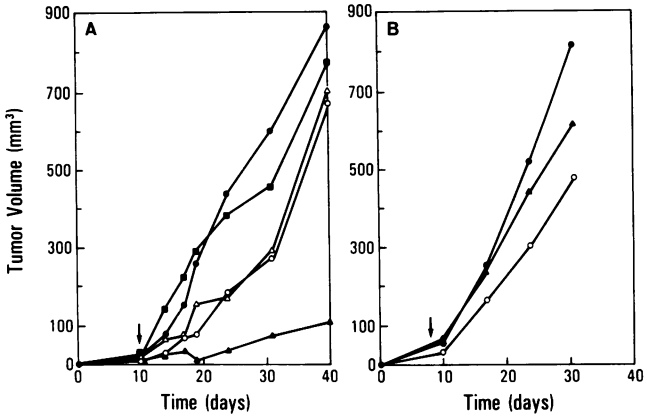

FIG. 4. Efficacy of DXR–mAb conjugates in suppressing tumor growth *in vivo*. M21 melanoma (*A*) and irrelevant UCLA-P3 lung tumor cells (*B*) were established as tumors in nude mice. Arrows indicate the first day of treatment for each tumor. Each animal was injected with a total dose of 75 μg of DXR i.v. during the following 30 days. ●, mAb 9.2.27 alone; ○, DXR alone; ▲, DXR–mAb 9.2.27; ■, DXR–mAb 11.4.1; △, unconjugated mixture of DXR and mAb 9.2.27. The tumor volume in the UCLA-P3 lung tumor group was monitored for the first 30 days only since the animals began to die at that time in all three treatment groups (*B*).

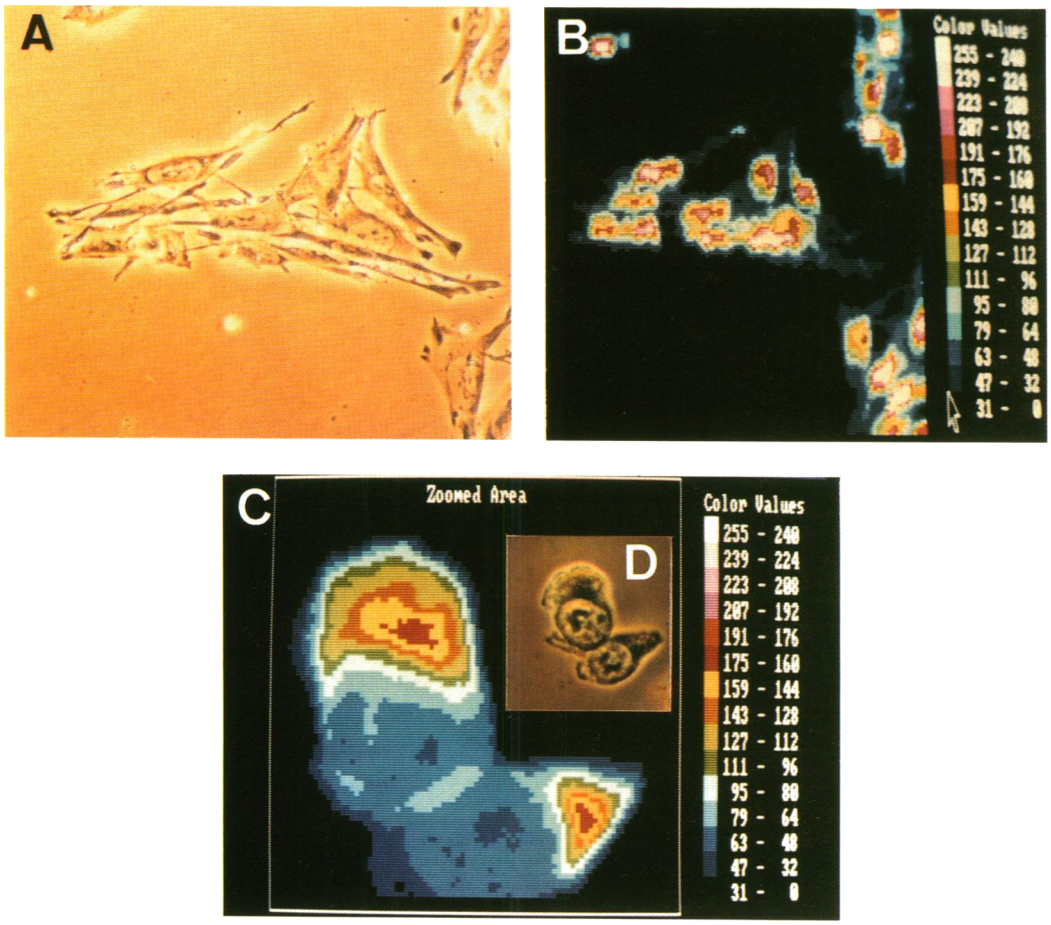

FIG. 3. Intracellular localization of DXR–mAb 9.2.27 conjugate in M21 cells. Melanoma cells were preincubated with 25 μM chloroquine for 1 hr at 37°C. DXR–mAb 9.2.27 conjugate was then added and incubated for another 2 hr. The cells were then analyzed with the ACAS 470 workstation. DXR molecules were found in the nuclei after 2 hr of incubation in the absence of chloroquine (*A*, phase contrast; *B*, fluorescence intensity of cells in the same field). In the presence of chloroquine, DXR-related fluorescence was concentrated at the perinuclear regions of M21 cells (*C* and *D*) and did not enter the nuclei.

Table 1. Effects of DXR–mAb conjugates on the survival of human tumor-bearing nude mice

Tumor	Treatment	% ILS*	Survivors at day 120/mice treated
Melanoma (M21)	mAb 9.2.27	0	0/10
	DXR	27	0/12
	DXR–mAb 9.2.27	81†	4/12
	DXR–mAb 11.4.1	−5	0/6
	mAb 9.2.27 + free DXR	−7	0/6
Lung adenocarcinoma (UCLA-P3)	mAb 9.2.27	−9	0/6
	DXR	−12	0/6
	DXR–mAb 9.2.27	7	0/6

*Percentage increase in life-span (ILS) on day 120 after tumor inoculum. The survival time of control mice treated with mAb 9.2.27 alone was 55 days.
†Mann–Whitney U test; $P < 0.01$.

was localized in the nuclei of M21 cells after 30 min incubation at 37°C (daa not shown). The nuclei-associated fluorescence in these cells was resistant to RNase but sensitive to DNase treatment, indicating that DXR was bound to nuclear DNA. Under identical conditions (30 min at 37°C), DXR–mAb 9.2.27 conjugates were predominantly observed in the cytoplasm. However, after a 2-hr incubation at 37°C, the majority of fluorescence was found in the nucleus (Fig. 3 *A* and *B*). This time lag required for the DXR–mAb 9.2.27 to enter the nucleus prompted an examination of the possible involvement of lysosomal degradation of DXR–mAb conjugates during this process. As expected, when the pH of the lysosomal compartment of M21 cells was increased by treatment with 25 μm chloroquine, the majority of fluorescence was localized in a perinuclear region of these cells after a 2-hr incubation with DXR–mAb 9.2.27 at 37°C (Fig. 3 *C* and *D*). In a control experiment, chloroquine treatment (25 μM) alone did not affect either the transport or DNA-binding ability of free DXR (data not shown).

DXR–mAb 9.2.27 Conjugates Specifically Suppress Tumor Growth *in Vivo*. The efficacy and specificity of DXR–mAb 9.2.27 conjugates to suppress tumor growth *in vivo* are shown in Fig. 4 and Table 1. Results indicated that only mice treated with DXR–mAb 9.2.27 conjugate demonstrated significant suppression of tumor growth in a tumor- and antibody-specific fashion—i.e., DXR–mAb 9.2.27 conjugates had no effect on the growth of the irrelevant UCLA-P3 tumors (Fig. 4*B*), which lack the 9.2.27 epitopes, and the irrelevant DXR–mAb conjugate, DXR–mAb 11.4.1, was ineffective against the melanoma tumors. In contrast, 8/12 M21 melanoma xenografts in the nude mice treated with the DXR–mAb 9.2.27 conjugates remained very small for the first 31 days after tumor inoculation and gradually increased in volume at a much slower rate than those in the other experimental groups (Fig. 4*A*). However, 4 of 12 mice in this same experimental group actually showed tumor regression and remained tumor free for the duration of the experiment. DXR treatment alone failed to significantly suppress the tumor growth of both M21 melanoma and UCLA-P3 lung adenocarcinoma in tumor-bearing mice (Fig. 4; $P > 0.1$). In addition, a mixture of mAb 9.2.27 and DXR also showed similar negative effects as DXR alone (Fig. 4*A*). The median survival time of animals treated with mAb 9.2.27 alone was 55 days; however, the life-span of animals receiving DXR–mAb 9.2.27 treatment was prolonged by 81% ($P < 0.01$) with 4 of 12 mice still surviving on day 120 (Table 1).

Biodistribution of Free DXR and DXR–mAb 9.2.27 Conjugates. The most striking finding was the preferential deposition of DXR in tumor delivered by DXR–mAb 9.2.27 as compared to that of freely administered drug (Table 2). In this case, except in bone, the deposition of freely administered DXR in the tissues decreased gradually within 48 hr. Only 0.8% of total injected [^{14}C]DXR was present in each g of M21 tumor, whereas 3.7% of total injected [^{14}C]DXR–mAb 9.2.27 was present in each g of M21 tumor. Thus, the immunoconjugate achieved a 4-fold increase of DXR in the target site as compared to that delivered by free DXR and DXR–mAb 11.4.1 48 hr postinjection. The other noticeable difference was that while 2.8% of total injected free DXR was localized in the bone 48 hr postinjection, only 0.5% of total injected DXR–mAb 9.2.27 was localized in the bone. The total deposition of DXR–mAb in M21 tumors remained stable between 24 hr (4.0%; data not shown) and 48 hr (3.7%) postinjection, while in the case of free DXR, the total dose decreased from 1.2% to 0.8%.

DISCUSSION

The results of this study demonstrate that conjugates of anti-melanoma mAb 9.2.27 with DXR are quite effective in specifically suppressing growth of established human melanoma xenografts in athymic (nu/nu) mice while markedly increasing the life-span of these animals. These results are remarkable since either mAb 9.2.27 or DXR *per se* failed to achieve such results and also because it is well known that human melanoma cells are resistant to this drug. In fact, previous phase I clinical trials with mAb 9.2.27 alone demonstrated excellent tumor targeting, but showed no effect at all on suppression of tumor growth (18). Also, in prior studies of athymic (nu/nu) mice bearing human melanoma xenografts, mAb 9.2.27 did not suppress growth of established tumors (5); however, simultaneous injection of this antibody with relatively large numbers (2.5×10^6) of mouse mononuclear splenocytes caused at least some tumor regression in this animal model system (19).

mAb 9.2.27 was chosen as a drug-targeting device for the present study because this antibody has several important characteristics. First, it targets melanoma cells most effectively. Second, the antibody has a very high affinity for

Table 2. Biodistribution of [^{14}C]DXR–mAb conjugates 48 hr postinjection

Organ	DXR		DXR–mAb 9.2.27		DXR–mAb 11.4.1	
	%ID/g ± SEM	T/B	%ID/g ± SEM	T/B	%ID/g ± SEM	T/B
Blood	0.7 ± 0.1	1.0	1.4 ± 0.3	1.0	3.8 ± 1.4	1.0
Tumor	0.8 ± 0.2	1.1	3.7 ± 0.5	2.6	1.0 ± 0.2	0.3
Skin	0.2 ± 0.0	0.3	0.5 ± 0.1	0.4	2.1 ± 0.8	0.6
Bone	2.8 ± 0.8	4.0	0.5 ± 0.1	0.4	1.0 ± 0.2	0.3
Lung	0.3 ± 0.1	0.5	1.8 ± 0.3	1.3	1.4 ± 0.3	0.4
Liver	1.4 ± 0.5	2.0	1.5 ± 0.4	1.1	3.2 ± 0.8	0.8
Spleen	1.0 ± 0.2	1.4	0.8 ± 0.2	0.6	1.9 ± 0.6	0.5
Kidney	1.4 ± 0.3	2.1	0.9 ± 0.1	0.6	2.7 ± 0.8	0.7
Intestine	1.1 ± 0.6	1.5	0.8 ± 0.1	0.6	1.6 ± 1.1	0.4

%ID/g, the percentage of injected dose per g of tissue; T/B, tissue/blood ratio.

melanoma cells ($K_a = 8 \times 10^9\ M^{-1}$). Third, mAb 9.2.27 does not cause antigen modulation *in vivo* and expression of the proteoglycan antigen recognized by it is not cell-cycle dependent (20). Most importantly, the results of phase I clinical trials indicated that mAb 9.2.27 administered i.v. in excess of 250 mg to melanoma patients effectively covered all skin lesions even though these tumors are known to have the least blood circulation (18). These properties of mAb 9.2.27 are particularly important for effective tumor targeting of DXR–mAb conjugates. Finally, the DXR–mAb 9.2.27 conjugates are stable in the circulation of nude mice for up to 48 hr, as revealed by $NaDodSO_4$/PAGE analysis of [^{14}C]-DXR–mAb 9.2.27 conjugates (data not shown).

It was most significant that 30 days after tumor-cell inoculation, four nude mice in the experimental group treated with DXR–mAb 9.2.27 conjugates still remained tumor free while the remaining eight animals developed only small lesions at a much slower rate than control animals (Fig. 4*A*). Mice treated with the DXR–mAb 9.2.27 conjugate also showed an 81% increase in life-span (Table 1). This improvement was considerably greater than that of 27% achieved with animals treated with DXR alone (Table 1). These data clearly demonstrate that growth of an established tumor can be markedly suppressed by the DXR–mAb 9.2.27 conjugates. Results of biodistribution studies further indicate that mAb 9.2.27 is able to deliver at least 4-fold more drug (3.7% of injected dose per g of tumor) than that of DXR in free drug form (0.8% of injected dose per g of tumor) to the tumor target (Table 2). Moreover, only free DXR, but not DXR–mAb 9.2.27 conjugates, was accumulated in the bone. Therefore, conjugated DXR showed overall far better localization indices than those obtained with free DXR. These data are consistent with the specific tumor suppression and increased life-span observed in the group of nude mice treated with DXR–mAb 9.2.27 (Fig. 4 and Table 1). Thus, DXR–mAb 9.2.27 conjugates effectively increase selective toxicity of free DXR. A similar result was obtained in a syngeneic mouse tumor model using methotrexate conjugated with an anti-EL4 lymphoma antibody, which localized well in EL-4 lymphoma in tumor-bearing mice 24 hr after i.p. injection (21).

The toxicity study in nude mice indicated that 400 μg of free DXR (two 200-μg injections at a 3-day interval) will kill 100% of animals within 6 days. In addition, the dose is cumulative in nude mice—i.e., four doses of 100 μg of free DXR will kill the mice within 14 days. Therefore, the dose used in this study, a total equivalent dose of 75 μg of DXR per mouse, can be significantly increased without toxicity. These data also indicate that our present drug delivery is still quite suboptimal and that even better results may be achieved under optimal conditions.

To gain some understanding of the mechanism(s) by which the DXR–mAb 9.2.27 conjugates suppress tumor growth, the initial binding, internalization, processing, and degradation of DXR–mAb conjugates was investigated in M21 melanoma cells. The fact that excess native mAb 9.2.27 can reverse the growth inhibition exerted by DXR–mAb 9.2.27 conjugates (data not shown) suggests that the immunoconjugate enters the tumor target cell via an antigen–antibody complex rather than by diffusion as has been proposed for free drug by other investigators (22). This hypothesis was further supported by a binding study in which [^{14}C]DXR–mAb 9.2.27 conjugates bound to M21 but not to control NMB-7 cells that do not express the 9.2.27 epitope (unpublished data). Taken together, these data suggest that DXR–mAb conjugates are effective only after they are internalized. Furthermore, the results from experiments conducted with chloroquine (Fig. 3) suggest that DXR–mAb 9.2.27 conjugate and free DXR follow different routes of degradation. Thus, free DXR bound to DNA within 30 min, whereas the DXR–mAb 9.2.27 conjugates remained in the cytoplasm, most likely in the endosomal or lysosomal compartments as previously suggested since chloroquine is known to selectively increase the intracellular pH of lysosomes and endosomes (8, 9). Passive uptake of drug through membranes or binding to drug receptors appears to be less likely, especially since DXR *per se* is ineffective in our system.

It is evident from our data that further investigations are required to optimize the efficacy of DXR–mAb 9.2.27 conjugates and to delineate their mechanism(s) of action.

We wish to thank Drs. A. Tramontano (Scripps Clinic) and W. Wrasidlo (Brunswick Biotechnology, San Diego) for helpful suggestions leading to the preparation of DXR–mAb conjugates. The technical assistance of Ms. W. Wiltse and the preparation of the manuscript by Ms. B. P. Filiault are greatly appreciated. This work was supported in part by a grant from the National Institutes of Health (CA 42508). H.M.Y. is the recipient of fellowships from Joseph Drown Foundation and the National Cancer Cytology Center. This is Scripps publication no. 4962-Imm.

1. Deguchi, T., Chu, T. M., Leong, S. S., Horoszewicz, J. S. & Lee, C.-L. (1986) *Cancer Res.* **46**, 3751–3755.
2. Lashfor, L., Jones, D., Gordon, I., Breatnach, F. & Kemshead, J. T. (1987) *Natl. Cancer Inst. Monogr.* **3**, 53–57.
3. Pastan, I., Willingham, M. C. & FitzGerald, D. J. (1986) *Cell* **47**, 641–648.
4. Bumol, T. F. & Reisfeld, R. A. (1982) *Proc. Natl. Acad. Sci. USA* **79**, 1245–1249.
5. Bumol, T. F., Wang, Q. C., Reisfeld, R. A. & Kaplan, N. O. (1983) *Proc. Natl. Acad. Sci. USA* **80**, 529–533.
6. Shen, W.-C. & Ryser, H. J.-P. (1981) *Biochem. Biophys. Res. Commun.* **102**, 1048–1054.
7. Diener, E., Diner, U. E., Sinha, A., Xie, S. & Vergidis, R. (1986) *Science* **231**, 148–150.
8. Sandrig, K. & Olsnes, S. J. (1980) *J. Cell Biol.* **87**, 828–832.
9. Pastan, I. & Willingham, M. C. (1983) *Trends Biochem. Sci.* **8**, 250–254.
10. Zunino, F., Gambetta, R., DiMarco, A. & Zaccara, A. (1972) *Biochim. Biophys. Acta* **277**, 489–498.
11. Ey, P. L., Prowse, S. J. & Jenkins, C. R. (1978) *Immunochemistry* **15**, 429–436.
12. Bradford, M. M. (1976) *Anal. Biochem.* **72**, 248–254.
13. Harper, J. R. & Orengo, A. (1980) *Anal. Biochem.* **113**, 51–57.
14. Mayhew, E. G., Goldrosen, M. H., Vaage, J. & Rustum, Y. M. (1987) *J. Natl. Cancer Inst.* **78**, 707–713.
15. Giuliani, F. C. & Kaplan, N. O. (1980) *Cancer Res.* **40**, 4682–4687.
16. Schneider, Y. J., Baurain, R., Zenebergh, A. & Trouet, A. (1979) *Cancer Chemother. Pharmacol.* **2**, 7–10.
17. Tobey, R. A., Crissman, H. A. & Oka, M. S. (1976) *Cancer Treat. Rep.* **60**, 1829–1834.
18. Oldham, R. K., Foon, K. A., Morgan, A. C., Woodhouse, C. S., Schroff, R. W., Abrams, P. G., Fer, M. F., Farrell, M. M., Kimball, E. S. & Sherwin, S. A. (1984) *J. Clin. Oncol.* **2**, 1235–1244.
19. Honsik, C. J., Jung, G. & Reisfeld, R. A. (1986) *Proc. Natl. Acad. Sci. USA* **83**, 7893–7897.
20. Lindmo, T., Rofstad, E. K., Fodstad, O. & Sundan, A. (1984) *Int. J. Cancer* **33**, 167–171.
21. Uadia, P., Blair, A. H. & Ghose, T. (1984) *Cancer Res.* **44**, 4263–4266.
22. Durand, R. E. & Olive, P. L. (1981) *Cancer Res.* **41**, 3489–3494.